Liquid Crystals
Publication details, including instructions for authors and subscription information:
http://www.informaworld.com/smpp/title~content=t713926090

A vector grouping algorithm for liquid crystal tensor field visualization

Yang-Ming Zhu; Paul A. Farrell

Online publication date: 06 December 2010

To cite this Article Zhu, Yang-Ming and Farrell, Paul A.(2002) 'A vector grouping algorithm for liquid crystal tensor field visualization', Liquid Crystals, 29: 10, 1259 — 1264
To link to this Article: DOI: 10.1080/713935624
URL: http://dx.doi.org/10.1080/713935624

LIQUID CRYSTALS, 2002, VOL. 29, NO. 10, 1259–1264

A vector grouping algorithm for liquid crystal tensor field visualization

YANG-MING ZHU* and PAUL A. FARRELL
Department of Computer Science, Kent State University, Kent, Ohio 44242, USA

(*Received 14 January 2002; accepted 26 June 2002*)

Tensor fields are at the heart of many science and engineering disciplines. Many tensor visualization methods separate the tensor into component eigenvectors and visualize those instead. Eigenvectors are normally ordered according to their eigenvalues: the eigenvectors corresponding to the smallest, median, or largest eigenvalues are in their corresponding groups. We show that this ordering strategy is undesirable for liquid crystal systems and propose a new approach, where the vectors are grouped to minimize some local energy. The grouping process is reminiscent of the epitaxial expansion in the anchoring of liquid crystals on a surface. The new algorithm is successfully applied to a liquid crystal system to study the biaxiality structure near a defect.

1. Introduction

Tensor data sets are at the heart of many science and engineering areas such as fluid dynamics, but few methods have been proposed to visualize and understand the richness of these fields [1, 2]. The first method proposed to visualize a tensor field is to represent the tensor by an ellipsoid, the orientations of which are determined by the eigenvectors, and the relative lengths of whose axes are determined by the eigenvalues [3]. The generalization of this approach is to use a local icon to represent the tensor at various points in space. As an alternative, scalar components can be analysed and displayed in 2D or 3D form, which is ineffective and may discard valuable information about the data. Motivated by their previous work on the topological representation of vector fields [4, 5], Hesselink and his co-workers recently proposed a topological approach [6, 7] which can capture the global structure of a tensor field.

A 3D tensor is a 3×3 matrix. A 3×3 matrix can be uniquely represented by three eigenvalues and their corresponding eigenvectors. The visualization of tensor fields thus can be reduced to the visualization of three vector fields, and any vector visualization method can be applied to these separated vector fields. In current practice [6, 7], the vector fields are separated according to their eigenvalues, i.e. eigenvectors corresponding to the largest eigenvalues are in a group, those corresponding to the median eigenvalues are in another group, and those corresponding to the smallest eigenvalues are in yet another group. The separated vector fields can be further processed as in the topological representation paradigm, where topological skeletons are emphasized [6]. A point where two or three eigenvalues are equal, is called degenerate. Tensor field lines or hyperstreamline trajectories are calculated in each separated vector field along those degenerate points. Those calculated topological skeletons can be rendered together or separately. This approach greatly reduces the display clutter and has proven to be useful in some areas.

In our research we found that the vector ordering strategy, i.e. separating eigenvectors according to the magnitude of the corresponding eigenvalues, is inappropriate for liquid crystal tensor field visualization. To remedy this, a vector grouping algorithm is developed in this paper based on the energy minimization principle. After the eigenvectors are properly grouped, any vector-rendering algorithms, including the topological skeletons, can be applied to the grouped vector fields.

The remainder of the paper is organized as follows. Section 2 describes the vector grouping algorithm with a brief discussion of its physics origin. Section 3 illustrates two examples to demonstrate that the conventional vector ordering scheme is inappropriate whereas the new strategy works well.

2. Vector grouping algorithm

Liquid crystals have different phases [8]. The nematic phase is studied most and is the focus of this paper. The orientation of liquid crystals can be abstracted by a

*Author for correspondence. Current address: Nuclear Medicine Division, Philips Medical Systems, 595 Miner Road, Cleveland, Ohio 44143, USA; e-mail: yzhu@computer.org

Liquid Crystals ISSN 0267-8292 print/ISSN 1366-5855 online © 2002 Taylor & Francis Ltd
http://www.tandf.co.uk/journals
DOI: 10.1080/0267829021000018068

director field **n**, a unit vector defined in space. The thermal average of **n** gives the director. If the director field is not a smooth function of spatial coordinates, the singular points and lines are called defects. For liquid crystals, **n** and $-\mathbf{n}$ are equivalent.

Traditionally liquid crystals are described by a vector field [8]. That implies that liquid crystals are uniaxial. However, experimental results indicate that liquid crystals may be biaxial [8, 9]. Theoretical results also show that, close to a topological defect, the liquid crystal is biaxial [10]. The vector representation is inadequate for this biaxial field. Instead a tensor field must be used.

The ordering of liquid crystals is described by the ordering matrix $Q^{\alpha\beta} = 1/2\langle 3n_\alpha n_\beta - \delta_{\alpha\beta}\rangle$, where $\alpha, \beta = x, y, z$ are indices referring to the laboratory frame, and δ is a Kronecker symbol defined as $\delta = 1$ if $\alpha = \beta$ and zero otherwise. In an explicit matrix form, $Q = 1/2\langle 3\mathbf{n}\mathbf{n}^{\mathrm{T}} - I\rangle$, where T indicates the transpose and I is a unit matrix. The tensor Q is traceless and symmetric. If all its eigenvalues are equal, it is an isotropic liquid. If two of them are equal, it is a uniaxial nematic. If none of them are equal, it is biaxial. Liquid crystals are uniaxial in most cases. Thus, in liquid crystal tensor field visualization, the uniaxial case is considered normal. If defects are involved, then some biaxial or isotropic regions are embedded in the uniaxial background. The changes of eigenvalues in space are also of interest.

The bulk free energy density of a liquid crystal system, according to the Landau–de Gennes theory, is

$$
\begin{aligned}
f_{\mathrm{bulk}} = {} & \frac{1}{2}L_1 Q_{\alpha\beta,\gamma} Q_{\alpha\beta,\gamma} + \frac{1}{2}L_2 Q_{\alpha\beta,\beta} Q_{\alpha\gamma,\gamma} + \frac{1}{2}L_3 Q_{\alpha\beta,\beta} Q_{\alpha\gamma,\beta} \\
& + \frac{1}{2}A\,\mathrm{tr}(Q^2) - \frac{1}{3}B\,\mathrm{tr}(Q^3) + \frac{1}{4}C\,\mathrm{tr}(Q^2)^2 \\
& + \frac{1}{5}D\,\mathrm{tr}(Q^2)\,\mathrm{tr}(Q^3) + \frac{1}{6}M\,\mathrm{tr}(Q^3)^2 + \frac{1}{6}M'\,\mathrm{tr}(Q^2)^3 \\
& - \Delta\chi H_\alpha Q_{\alpha\beta} H_\beta - \Delta\varepsilon E_\alpha Q_{\alpha\beta} E_\beta
\end{aligned}
$$

where traditional physics conventions are used, i.e. summation over repeated indices is implied and indices separated by commas indicate partial derivatives with respective to the index after the comma. Here, L_1, L_2, L_3, A, B, C, D, M, M', H, E, $\Delta\varepsilon$, $\Delta\chi$ are physical constants.

To find the stable configuration of a liquid crystal system, one needs to minimize the Landau–de Gennes energy numerically. The computation of this system is challenging. It is desirable to implement the solver on a parallel machine, or on a distributed network of workstations. The solver has already been implemented, in the Department of Computer Science at Kent State University, on a 16 384 processor 512 Mbyte memory Wavetracer DTC SIMD machine for a 2D slab geometry, and on a distributed network of workstations using MPI (Message Passing Interface).

The visualization of tensor fields can be reduced to the visualization of three vector fields. To visualize these vector fields, they first have to be grouped. The idea of our vector grouping algorithm is to minimize the direction change in each vector group. For two unit vectors, if their directions differ slightly, their inner product has a large value (close to 1). Assume eigenvalues λ_1, λ_2, and λ_3 and their corresponding unit eigenvectors u, v, and w are given in space (x_i, y_j, z_k), $i, j, k = 0, 1, \ldots, N-1$. The algorithm intends to group vectors along a line, grow the ordering in a plane and then into the bulk. It has the following steps:

(1) At (x_0, y_0, z_0), pick three eigenvectors arbitrarily and label them as $U_{0,0,0}$, $V_{0,0,0}$, and $W_{0,0,0}$.

(2) For $i = 1, 2, \ldots, N-1$, and for the six permutations of eigenvectors $(U_{i,0,0}, V_{i,0,0}, W_{i,0,0})$: (u, v, w), (u, w, v), (v, u, w), (v, w, u), (w, u, v), or (w, v, u), compute

$$
(U_{i-1,0,0}, U_{i,0,0})^2 + (V_{i-1,0,0}, V_{i,0,0})^2 + (W_{i-1,0,0}, W_{i,0,0})^2
$$

where (a, b) is the inner product of vector a and b. Pick the permutation that has the largest value and swap the involved eigenvalues and eigenvectors accordingly. For example, if (w, u, v) gives the largest value, then swap u and w first and then swap u and v.

(3) For $i = 0, 1, \ldots, N-1$, $j = 1, 2, \ldots, N-1$, and for the six permutations of (U, V, W) at (x_i, y_j, z_0), compute

$$
\sum_{\langle x,y\rangle} (U_{x,y,0}, U_{i,j,0})^2 + (V_{x,y,0}, V_{i,j,0})^2 + (W_{x,y,0}, W_{i,j,0})^2
$$

where $\langle x, y\rangle = (i-1, j-1), (i, j-1), (i+1, j-1)$. Pick the permutation that has the largest value and swap the involved eigenvalues and eigenvectors accordingly. If some neighbours of (x_i, y_j, z_0) are missing, the associated terms are dropped out.

(4) For $i = 0, 1, \ldots, N-1$, $j = 0, 1, \ldots, N-1$, $k = 1, 2, \ldots, N-1$, and for the six permutations of (U, V, W) at (x_i, y_j, z_k), compute

$$
\sum_{\langle x,y,z\rangle} (U_{x,y,z}, U_{i,j,k})^2 + (V_{x,y,z}, V_{i,j,k})^2 + (W_{x,y,z}, W_{i,j,k})^2
$$

where $\langle x, y, z\rangle = (i-1, j-1, k-1), (i, j-1, k-1), (i+1, j-1, k-1), (i-1, j, k-1), (i, j, k-1), (i+1, j, k-1), (i-1, j+1, k-1), (i, j+1, k-1), (i+1, j+1, k-1)$. Pick the permutation that has the largest value and swap the involved eigenvalues and eigenvectors accordingly. If some neighbours of (x_i, y_j, z_k) are missing, the associated terms are dropped out.

In step (2) the ordering grows along a line. In step (3) the ordering grows from a line. In step (3) one may group the vectors in two edges and then grow the ordering into the bulk, or group around the four edges first, then shrink to the centre. In step (4) the ordering grows from a plane. All the nine neighbours from the previous plane of the current point are considered. Alternatively, for simplicity, one may just consider five neighbours $(i, j, k-1)$, $(i-1, j, k-1)$, $(i+1, j, k-1)$, $(i, j+1, k-1)$, and $(i, j-1, k-1)$. Again, there are other alternatives, involving grouping the vectors along different planes and from different corners.

Since u and $-u$ are both eigenvectors of the corresponding eigenvalue, we compute the squared inner products while grouping. If, while grouping, one wants to take into account the eigenvalues, $\lambda_{U_{i-1}}\lambda_{U_i}(U_{i-1}, U_i)^2$ or a similar expression can be used. We also found that, if the absolute value of the inner product is used, similar results can be achieved.

Our algorithm has a physical basis. For an Ising model with two spin states (up and down), the Hamiltonian is [11]

$$H = -J \sum_{\langle i,j\rangle} S_i \cdot S_j$$

where positive J is the molecular interaction, and S_i is the spin on lattice i. If the state is a vector, then

$$H = -J \sum_{\langle i,j\rangle} (v_i, v_j)$$

where v_i is the vector state on lattice i. For a liquid crystal system, in particular [12],

$$H = -J \sum_{\langle i,j\rangle} (v_i, v_j)^2$$

since $-\mathbf{v}$ and $\mathbf{v}$ are equivalent. Similarly, if the state is described by a tensor, we define a Hamiltonian as

$$H = -J \sum_{\langle i,j\rangle} (u_i, u_j)^2 + (v_i, v_j)^2 + (w_i, w_j)^2$$

where u_i, v_i, w_i are the eigenvectors on lattice i. To find the most favourable state, this Hamiltonian can be minimized, which is the same as the maximization criterion used in the grouping algorithm. It is worth noting that the approach used in the grouping algorithm is similar to the epitaxial growth of liquid crystals on a surface [13].

3. Examples and discussion

In this section, we show two examples of the application of the vector grouping algorithm to liquid crystal tensor field visualization.

A 2D data set was generated on a SIMD machine by implementing a numerical solver for the Landau–de Gennes model (see § 2 for details). The scaled temperature was 0.65 and the data set size was 65×65. Two defects of strength 1/2 were introduced in the calculation.

Figure 1 shows the rendering result, when eigenvectors are separated based on the relative strength of their eigenvalues: eigenvectors corresponding to the largest, medium, and smallest eigenvalues are rendered to the right, middle and left viewports, respectively. In the following examples, the viewports and eigenvalues have the same relation, when the eigenvectors are ordered based on their eigenvalues. To reduce display clutter, only the vectors on every other grid line in each dimension are displayed.

In the right viewport, the defects (singular points) introduced in the calculation are obvious and labelled with crosses. Those defects are also visible in the left viewport (but not labelled). The other four crosses labelled in the left viewport are artifacts due to the grouping scheme used. Similar artifacts are also visible in the middle viewport, at the corresponding positions close to the four corners. The distortion is more pronounced in an orthogonal projection with a stride of 1. These distortions are not favourable energetically. In fact, at these corners, the biaxiality is weak and we would not expect such a big distortion. Figure 2 shows the rendering results using our grouping algorithm. The situation in the four corners is significantly improved. Our new grouping strategy eliminates the false defects.

The eigenvalues are colour coded in figures 1 and 2. From the right and left viewports, one can clearly observe that the eigenvalues decrease close to the defects. Since eigenvalues reflect the ordering of the field, the ordering decreases on approaching the defects.

A 3D data set was generated by a cluster of workstations, which implements the solver for the 3D case. The size of this data set was $21 \times 21 \times 21$. The scaled temperature was 0.328. Currently, we are unable to generate bigger data sets, such as $100 \times 100 \times 100$. A defect, with strength one, was introduced at the centre of the field during the computation. Homeotropic surface

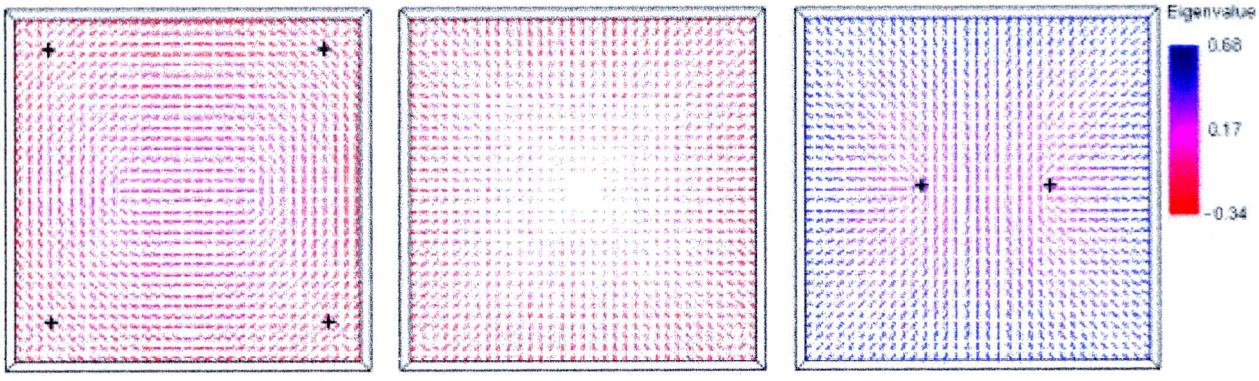

Figure 1. A 2D tensor field, with two defects, rendered according to the relative strength of eigenvalues. The stride is 2.

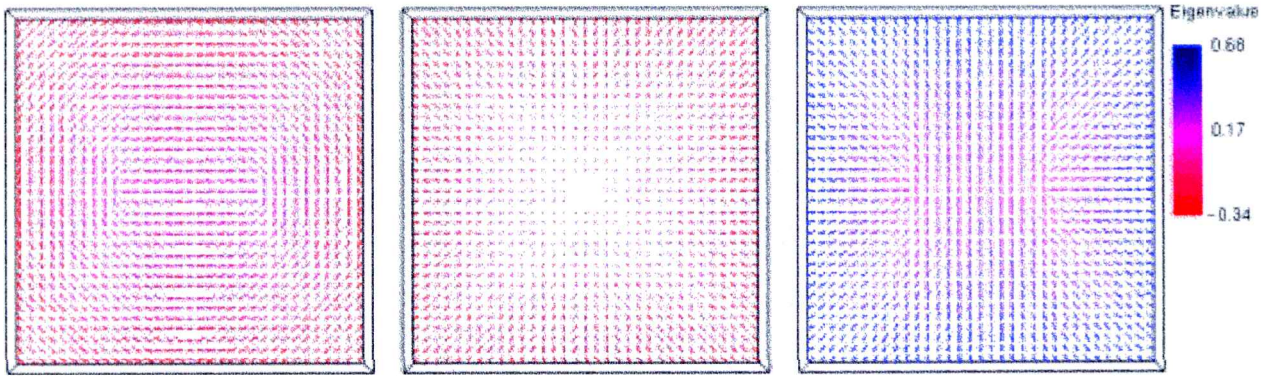

Figure 2. The same 2D tensor field as in figure 1, rendered using the vector grouping algorithm. The stride is 2.

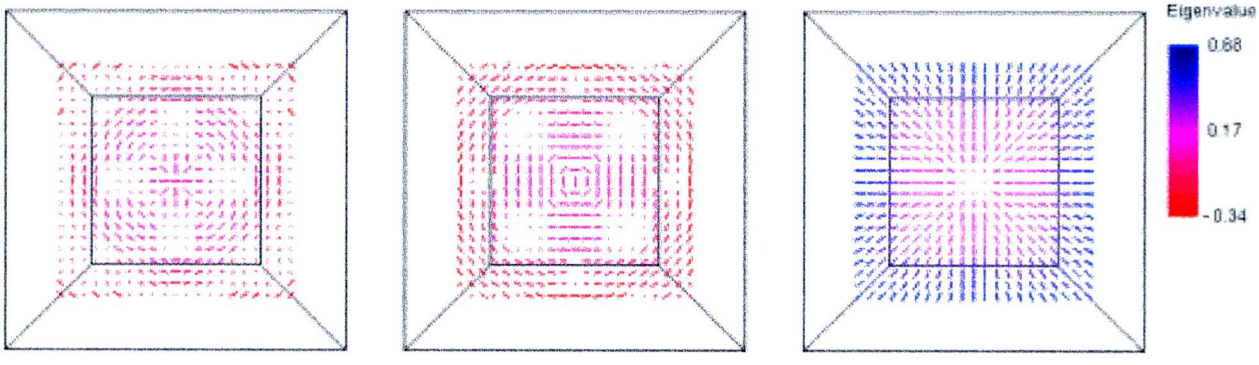

Figure 3. A 3D tensor field rendered according to the magnitude of the eigenvalues. The 12th slice parallel to the XOY plane is displayed.

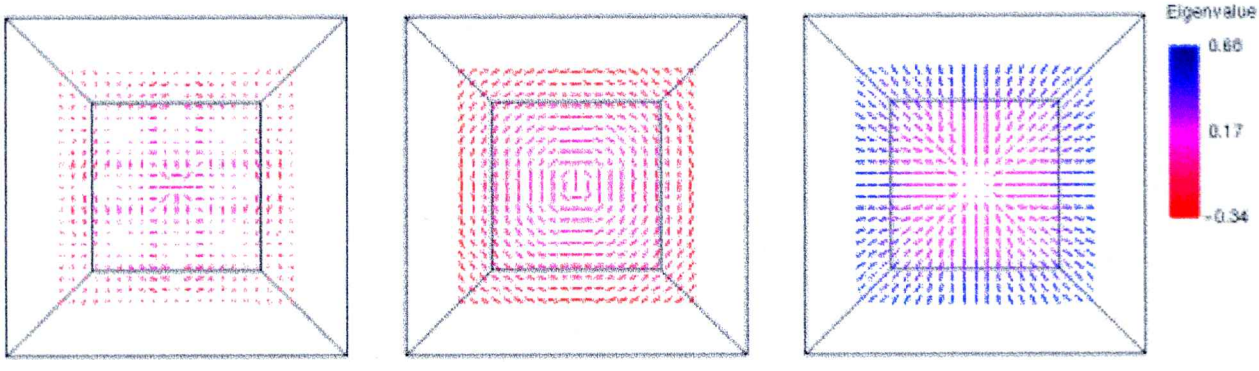

Figure 4. The same 3D tensor field as in figure 3 rendered with the vector grouping algorithm.

anchoring conditions were assumed; that is, all major eigenvectors are perpendicular to the surface and, more or less, they are in the radial direction in the bulk.

Figure 3 shows the vector fields at the 12th slice parallel to the XOY plane. The eigenvectors are separated according to the magnitude of their eigenvalues. Since the defect is at the centre of the field (in the 10th slice), we expect to see no defects, which is confirmed by the major vector component in the right viewport. The major eigenvectors are perpendicular to the paper surface in the centre and tilt gradually until parallel to the paper surface towards the confining boundary. The ordering decreases close to the defect. The rendering in the left and middle viewports is physically unacceptable. Along the surface, these vector fields should have a more or less regular configuration by a simple symmetry argument. In the bulk, the change of vector direction should be smooth. In the left and middle viewports of figure 3, however, the discontinuity of the vector fields along the edge and in the bulk is evident.

Figure 4 shows the rendering of the same slice, where vector fields were grouped using the vector grouping algorithm. The vectors in the central plane (10th plane) were grouped first and then grown in the two opposite directions in Z. In all these calculations, eigenvalues were also taken into account as we discussed earlier. There is no difference detected in the right viewport, but the renderings of the left and middle viewports are noticeably different. Unlike the vectors in figure 3, the vectors along the edges exhibit a regular pattern in both the left and middle viewports. The regularity of the vector field in the middle viewport is greatly improved compared with that in figure 4. The regularity of the vectors in the left viewport is also arguably improved. Some irregularity in the left viewport is due to the effect of projection. If the vectors in the irregular region are replaced by those in the middle viewport at the corresponding positions, the irregularity still exists. The data set used here is relatively small and the direction changes of vectors in each group is relatively large, thus this effect of projection is inevitable. However, there are vectors still misgrouped, e.g. the vector immediately above the vector at the centre. This misgrouping is difficult to avoid due to the limited amount of data points and the rapid change of direction between neighbouring data points. Moreover, as the distance to the initial plane becomes large, the separated eigenvectors become random. Nevertheless, our grouping scheme reduces the amount of irregularity in the grouped vector fields and gives a reasonable result.

The grouping result of our algorithm may depend on the direction in which the ordering grows. In fact our algorithm is a special implementation of the energy minimization principle. In this implementation, the neighbours, whose vectors have not been grouped, are not considered. An ideal implementation is to consider all neighbours, using a Monte Carlo type method, which is much slower than the scheme presented here. If the grouping direction dependency is a problem, one can resort to a Monte Carlo method. In the case of liquid crystals, the orientation is imposed by the surface contacting them. Therefore growth from a particular direction seems appropriate

4. Conclusion

A 3×3 tensor can be uniquely expressed by three eigenvalues and their corresponding eigenvectors. The visualization of the tensor field is equivalent to the visualization of three eigenvector fields, without loss of any information. We have shown that it is not appropriate to separate the eigenvectors of liquid crystal tensor fields based on the relative strength of their eigenvalues and then render these eigenvector fields. A vector grouping strategy is proposed to minimize the directional changes in each vector group. This strategy has been successfully applied to grouping eigenvectors of 2D and 3D tensor fields. The grouped eigenvectors make sense from a physics standpoint, and any vector visualization techniques, including local icon depiction and streamline representation, can be subsequently used to render the grouped eigenvector fields.

Thanks are due to Dr Arden Ruttan, for providing the 3D data set. This work was supported by the National Science Foundation under grant No. 9720221, by the NSF Advanced Liquid Crystalline Optical Material (ALCOM) Science and Technology Center, and by an Ohio Board of Regents Research Challenge grant.

References

[1] Nielson, G. M., Hagen, H., and Muller, H., 1997, *Scientific Visualization: Overviews, Methodologies, and Techniques*, edited by Los Alamitos (CA: IEEE Computer Society Press), Chap. 13, 16, 21.

[2] Livingston, M. A., 1997, *Proc. IEEE Visualization'97*, 491.

[3] Hesselink, L., and Delmarcelle, T., 1994, *Scientific Visualization: Advances and Challenges* (IEEE Computer Society Press), Chap. 26.

[4] Helman, J., and Hesselink, L., 1989, *Computer*, August, pp. 27–36.

[5] Helman, J., and Hesselink, L., 1991, *IEEE Computer Graphics and Applications*, **11,** 36.

[6] Hesselink, L., Levy, Y., and Lavin, Y., 1997, *IEEE Trans. Visualization and Computer Graphics*, **3,** 1.

[7] Lavin, Y., Levy, Y., and Hesselink, L., 1997, *Proc. IEEE Visualization'97*, 59.

[8] STANLEY, H. E., 1971, *Introduction to Phase Transitions and Critical Phenomena* (Oxford: Clarendon Press).
[9] LEBWOHL, P. A., and LASHER, G., 1972, *Phys. Rev. A*, **6,** 426.
[10] FANG, J. Y., LU, Z. H., MIN, G. W., AI, Z. M., WEI, Y., and STROEVE, P., 1992, *Phys. Rev. A*, **46,** 4963.
[11] DE GENNES, P. G., and PROST, J., 1993, *The Physics of Liquid Crystals*, 2nd Edn (Oxford Univ. Press).
[12] CHANDRASEKHAR, S., NAIR, G. G., RAO, D. S. S., PRASAD, S. K., PRAEFCKE, K., and BLUNK, D., 1998, *Liq. Cryst.*, **24,** 67.
[13] SCHOPOHL, N., and SLUCKIN, T. J., 1987, *Phys. Rev. Lett.*, **59,** 2582.